Four-step pulses of fractional-order surface plasmons

Yuping Yang[1,2] and D. Grischkowsky[2,*]

[1]*School of Science, Minzu University of China, Beijing 100081, China*

[2]*School of Electrical and Computer Engineering, Oklahoma State University, Stillwater, Oklahoma 74078, USA*

**Corresponding author: daniel.grischkowsky@okstate.edu*

Received March 6, 2012; accepted March 23, 2012;
posted March 30, 2012 (Doc. ID 164224); published May 14, 2012

The 0-order transmission of a 1D metallic grating, on a high-resistivity silicon wafer in optical contact with a silicon plate, has been characterized by terahertz time-domain spectroscopy with subpicosecond resolution over a 400 ps scan range. Two new long-time-delay, powerful pulses are observed after the second reflected pulse. In the frequency domain, these two strong and fast-ringing structures correspond to the bandwidth ranges between the [0, 1] and [0, 2] surface plasmon modes and the range above [0, 2], respectively. A physical optics ray analysis provides an intuitive understanding of these new four-step (reflection, diffraction, total reflection, and diffraction) pulses, caused by fractional-order surface plasmon type beam coupling.

OCIS codes: 240.6680, 300.6495, 050.6624.

Recently, a new type of extremely sharp resonant lines between the fundamental surface plasmon (SP) modes of a hole array fabricated on high-resistivity silicon wafers in "optical contact" with thick silicon plates was reported and identified as fractional-order surface plasmons (FSP) [1]. More recently, based on the study of a 1D metallic grating, we have shown experimentally that the FSP resonances are caused by the surprisingly large reflections due to gaps as thin as 1 μm between the backside of the hole array wafer and the thick backing plate [2]. The reflection from these gaps couples the strong 1-order diffracted beams into the 0-order beam causing the FSP oscillations.

We show in Fig. 1 that even when the gap is eliminated and the associated FSP oscillations on the 0-order transmitted pulse $T1$ disappear; very strong, much delayed, chirped, and long-lasting pulses are observed after the second reflected pulse $R2$ of the 0-order beam. These pulses are caused by a new four-step process, which couples 1-order diffracted beams into the 0-order beam. These four-step (reflection, diffraction, total reflection, and diffraction [RDRD]) pulses provide additional physical insight into the FSP-type beam coupling mechanisms, since they are distinguished by their time of arrival due to different round trip paths. A physical optics (PO) ray model is employed to identify the different sources of diffraction for these temporally isolated signals.

Figure 1(b) shows the temporal oscillations of the first 0-order transmitted pulse ($T1$) in more detail, where the clean ring-down signal indicates complete optical contact. The corresponding amplitude spectrum of the $T1$ pulse is shown in the inset and clearly shows the two fundamental SP resonances with no FSP oscillations.

The 1D grating with a period of 100 μm, with 75 μm Al lines separated by 25 μm, is schematically shown in Fig. 1(a). The 280 nm-thick Al film grating was fabricated by photolithography on a double-side polished 0.36 mm-thick high-resistivity Si wafer. A 3 mm-thick, high-resistivity Si plate was placed in optical contact with the backside of the grating wafer to eliminate the wafer backside reflection. The THz input pulses were linearly polarized (horizontal) and at normal incidence to the vertical lines of the grating.

The second reflected pulse ($R2$), shown in Fig. 2(a), is followed by two strong ringing pulses, RDRD-I and RDRD-II, in the time zones TZ0, TZ1, and TZ2, respectively. The corresponding fast Fourier transform (FFT) amplitude spectra of the transmitted THz signal in these three regions are shown in Fig. 2(b). The TZ0 spectrum is mainly below the fundamental [0, 1] SP mode at 0.88 THz, while the TZ1 spectrum is predominantly above the fundamental [0, 2] SP mode at 1.76 THz; the TZ2 spectrum is

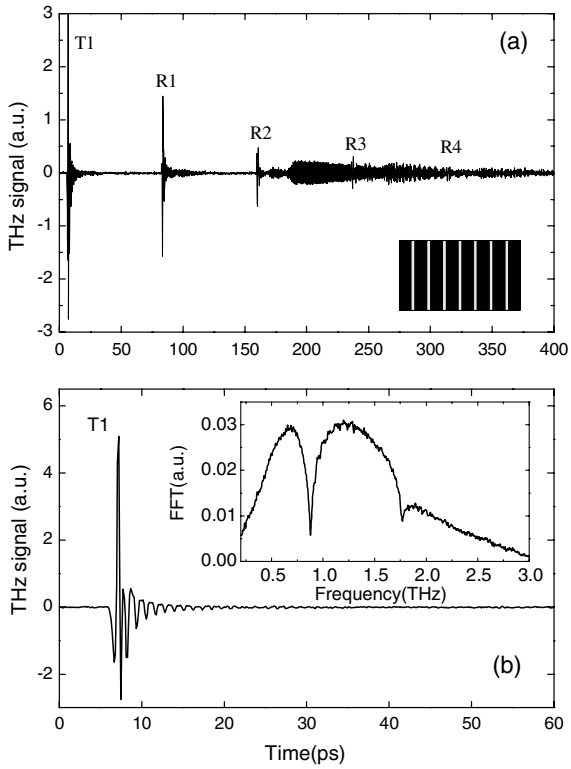

Fig. 1. (a) Measured transmitted THz pulses through the 1D grating in contact with a 3 mm Si backing plate in range of 0–400 ps with subpicosecond time resolution [3]. The first 0-order transmitted pulse is labeled as $T1$, and the reflections for the 0-order diffraction between the back surface of the Si plate and the front surface of the Si wafer are labeled as $R1$, $R2$, $R3$, and $R4$; (b) $T1$ is shown in the range of 0–60 ps, with the corresponding amplitude spectrum shown in the inset.

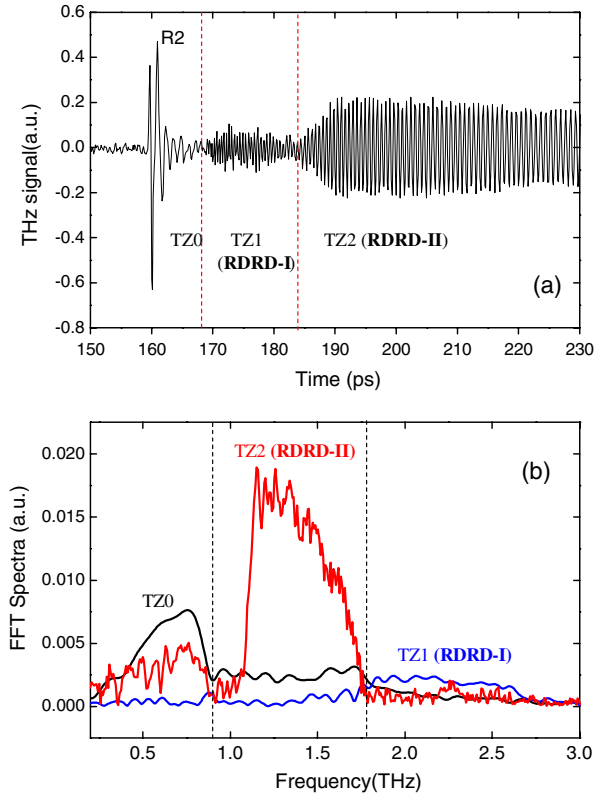

Fig. 2. (Color online) (a) Measured R2 and RDRD pulses shown in the range of 150–230 ps with an expanded vertical scale referenced to Fig. 1. The dashed vertical lines mark 168.5 and 184 ps; (b) amplitude transmission spectra of the three time zones of (a). The dashed vertical lines mark 0.88 and 1.76 THz.

mainly between the fundamental [0, 1] and [0, 2] SP modes; the FFT for the RDRD-II pulse was extended to 260 ps for more accuracy.

We now apply the PO ray model to explain the well-resolved individual features of the time-domain data. Figure 3 is a cross-sectional diagram describing the four-step RDRD effect. The 0-order transmission directly passes through the grating and plate assembly. The reflection of the 0-order ray at the output face is the first

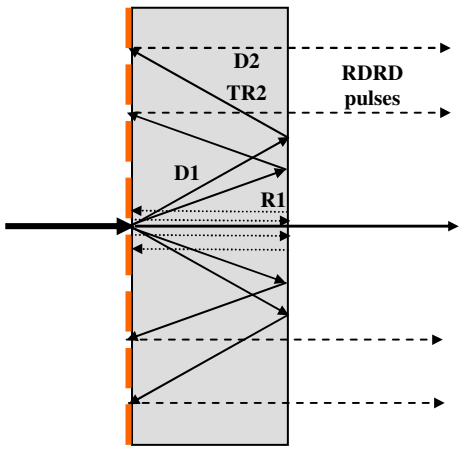

Fig. 3. (Color online) Cross-section diagram showing the 0-order transmission and the four-step path of RDRD pulses to the 0-order transmission direction for two different wavelengths.

reflection shown as ray $R1$, which is then diffracted by the reflective grating as ray $D1$, which in turn is totally reflected at the output face, as ray TR2, which is then diffracted in the forward 0-order direction, and is shown by the dashed line ray $D2$.

In our collinear mounting ($\theta_i = 0$), the 1-order diffraction angle is $\theta_1 = \arcsin(\lambda_0/nP)$, and for the weaker 2-order diffraction $\theta_2 = \arcsin(2\lambda_0/nP)$, with λ_0 the free-space wavelength, P the grating periodicity (100 μm), and $n = 3.42$. The diffraction angle θ tracks wavelength, with the longer wavelengths appearing at larger angles [2]. The fundamental [0, 1] SP mode of the periodic structure has the free-space wavelength $\lambda_{sp} = nP$, and frequency of 0.88 THz [4,5]. Therefore, 1-order diffraction occurs at frequencies above the fundamental [0, 1] SP mode at 0.88 THz and for frequencies below 3 THz at angles beyond the critical angle $\theta_c = \arcsin(1/n) = 17.0°$. Correspondingly, 2-order diffraction occurs at frequencies above the fundamental [0, 2] SP mode at 1.76 THz. The ray diagram in Fig. 3 for 1-order would be the same for 2-order with twice the frequency.

Based on the PO ray model, the three time regions of the measured $R2$ pulse and the following RDRD pulses in Fig. 2(a) can be explained: the first part of the THz pulse in TZ0 is the second reflection $R2$ of the 0-order diffraction with the frequencies overlapping the range of the transmitted pulse. The second part of the THz pulse in TZ1 is the first RDRD-I pulse with frequencies higher than the [0, 2] SP mode, and the third part of the THz pulse in TZ2 is the second RDRD-II pulse with frequency components between the [0, 1] and [0, 2] SP modes, except for the small feature at 2.25 THz, considered to be due to the transform of the RDRD-II pulse overlapping the small $R3$ reflection. Consequently, the 2-order diffraction for frequencies higher than 1.76 THz is considered to be negligible. The lower-frequency RDRD-II pulse arrives much later and lasts much longer because of the much longer round-trip distance due to bigger diffraction angles and its wider range. This result is consistent with the 1-order path increasing with wavelength, as shown as Fig. 3.

By applying the RDRD ray diagram to the 1-order diffraction, it can be seen that the optical path lengths of the RDRD pulses are completely defined by $L_{\mathrm{RDRD}} = 2h(1 + 1/\cos\theta_1)$, with h the thickness of Si plate plus the wafer ($h = 3.36$ mm), θ_1 the diffraction angle, and $n = 3.42$. L_{RDRD} can be rewritten as $L_{\mathrm{RDRD}} = 4h + 2h[(1/\cos\theta_1) - 1] = L_D + L_{\mathrm{DD}}$, where L_D describes the simple $4h$ delay and L_{DD} describes the wavelength dependent dispersive delay. From the time separation for the isolated pulses, their propagation will be determined more precisely from the following frequency-domain analysis.

Using the $T1$ pulse as the complex input wave $E_{T1}(\omega)$ and following the PO model, the complex amplitude of the RDRD pulse is calculated by

$$E_{\mathrm{RDRD}}(\omega) = E_{T1}R_1R_{D1}R_{\mathrm{TR}}R_{D2}\exp[i(2\pi f n/c)(L_D + L_{\mathrm{DD}})], \quad (1)$$

where the total reflection coefficient R_{TR} is 1, R_1 is the reflection coefficient at the Si–air interface;

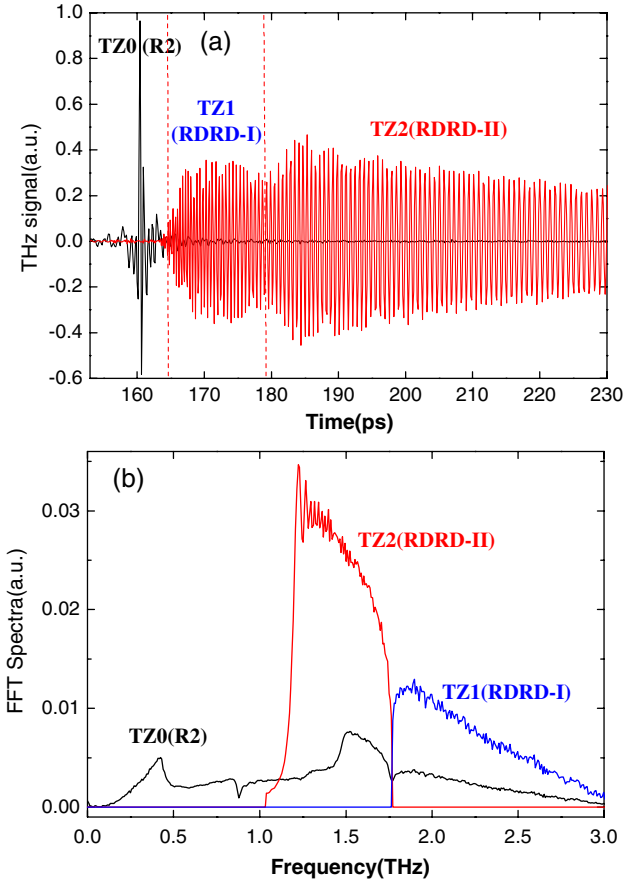

Fig. 4. (Color online) (a) Calculated RDRD pulse in range of 150–230 ps with an expanded vertical scale referenced to Fig. 1. The dashed vertical lines mark 164 and 178 ps. (b) Amplitude transmission spectra of three time zones of (a).

$R_1 = (n-1)/(n+1) = 0.547$. R_{D1} and R_{D2} are the single-slit diffraction functions at the Si–grating interface. For this proof of concept evaluation, R_{D1} and R_{D2} are set equal to unity.

For the $R2$ pulse, mainly in region TZ0, the complex amplitude can be written in a similar, but simpler form as

$$E_{R2}(\omega) = E_{T1} R_1^2 R_G^2 \exp[i(2\pi f n \cdot L_D/c)]. \quad (2)$$

$R_G(\omega)$ is the theoretical complex reflection coefficient at the Si–grating interface, which agrees well with the experimentally determined complex ratio $E_{R1}(\omega)/E_{T1}(\omega) = R_G(\omega)R_1$. Both E_{RDRD} and E_{R2} have experienced a reflection from the Si–air interface.

As shown in Fig. 4(b), the spectral amplitudes of the RDRD pulses are higher than that of $R2$, because R_D and R_{TR} are larger than R_G and R_1. Similar to the experimental observation in Fig. 2(b), the frequency components between the fundamental [0, 1] and [0, 2] SP modes are much stronger than those below the fundamental [0, 1] SP mode. For the numerical evaluation of $E_{\mathrm{RDRD}}(\omega)$, the amplitude of $E_{T1}(\omega)$, below 1.0 THz was set to zero to prevent large unobservable diffraction angles and imaginary diffraction angles.

The $R2$ pulse together with the RDRD pulses plotted in Fig. 4(a) were obtained by taking IFFT of $E_{\mathrm{RDRD}}(\omega)$ and $E_{R1}(\omega)$. Note that the calculated $R2$ pulse peaks at 160 ps (160 ps), and that the RDRD-I and II pulses start at 164 ps (168.5 ps) and 178 ps (184 ps), where the experimental values from Fig. 2(a) are given in parentheses. These values are referenced to the $T1$ pulse of Fig. 1(b), which starts at 6 ps. The agreement is considered satisfactory and confirms that the PO ray model is a good approximation for explaining the observations.

Overall, we have provided an intuitive understanding of the formation of the new powerful RDRD pulses and have now shown that for both hole arrays [2] and gratings, the study of SP effects by measuring the 0-order transmission must also take into account the FSP coupling processes for 1-order diffraction beams. The four-step process, powerful, long-duration, and frequency-chirped RDRD-II pulses present new challenges and opportunities for THz science and technology, as shown by the following two examples.

The large group velocity dispersion of the RDRD effect, where the longest wavelengths go the slowest, is ideal for recompressing THz pulses broadened by passage through a dielectric waveguide, where the longest wavelengths go the fastest, because of the fringing fields. The fact that the RDRD-II pulse has been frequency-chirped and broadened to more than 100 ps with a precise correspondence between time position and frequency enables spectroscopic frequency measurements in the time domain.

We acknowledge experimental support from S. Sree Harsha and Alisha J. Shutler, and numerical analysis support from Qi Cheng, Mahboubeh Mandehgar and Yihong Yang. This work was supported by the U.S. National Science Foundation (NSF), the National Natural Science Foundation (NSFC) (grant 11104360) and the "985 Project" (grant no. 98507-010009) and "211 project" of Ministry of Education of China.

References

1. D. Qu and D. Grischkowsky, Phys. Rev. Lett. **93**, 196804-1 (2004).
2. Y. Yang and D. Grischkowsky, Opt. Lett. **36**, 4218 (2011).
3. D. Grischkowsky, S. Keiding, M. van Exter, and Ch. Fattinger, J. Opt. Soc. Am. B **7**, 2006 (1990).
4. T. W. Ebbesen, H. J. Lezec, H. F. Ghaemi, T. Thio, and P. A. Wolff, Nature **391**, 667 (1998).
5. D. Qu, D. Grischkowsky, and W. Zhang, Opt. Lett. **29**, 896 (2004).